UNIVERSITY OF CALIFORNIA SAN DIEGO

Neural Activity in Rat Orbitofrontal Cortex Related to Punishment and Reward

A thesis submitted in partial satisfaction of the
requirements for the degree Master of Science

in

Biology

by

Tianzhi Tang

Committee in charge:

Professor Dhakshin Ramanathan, Chair
Professor Eric Bennett, Co-chair
Professor Ashley Juavinett

2020

The Thesis of Tianzhi Tang is approved, and it is acceptable in quality and form for publication on microfilm and electronically:

_____

_____

Co-Chair

_____

Chair

University of California San Diego

2020

DEDICATION

I'd like to dedicate my thesis to:

My parents, Yi Tang and Jin Fu, for their continuous support of my education.

My girlfriend, Victoria Shi, for her love and support throughout my undergraduate and master's years.

My PI, Dr. Dhakshin Ramanathan and postdoc, Dr. Miranda Francoeur, for their patient instructions and thoughtful guidance.

Undergraduate students in my lab (Sidharth Hulyalkar, Alyssa Terry, Chris Claros, Anona Gupta, and Xuanyu Wu) for their help on conducting behavioral trainings for rats and data analysis.

TABLE OF CONTENTS

LIST OF FIGURES

LIST OF ABBREVIATIONS

ACC	Anterior cingulate cortex
BOLD	Blood-oxygen-level dependent
EIB	Electrode interface boards
LFP	Local field potential
MDD	Major depressive disorder
SUD	Substance abuse disorder
OCD	Obsessive-Compulsive Disorder
OFC	Orbitofrontal cortex
RPE	Reward-prediction error

ACKNOWLEDGEMENTS

I would like to acknowledge my mentors, Dhakshin Ramanathan and Dr. Miranda Francoeur, for their continuous patience, guidance, and trust. Their support along this journey is paramount and I am forever grateful to be a part of the NEATLabs.

I would also like to acknowledge my committee members, Dr. Eric Bennett and Dr. Ashley Juavinett, for their interest in my project.

Chapter 1 of the results and discussion is currently being prepared for submission for publication of the material. T. Tang, M. Francoeur, D. Ramanathan. The thesis author is the primary author of this material.

Chapter 2 of the results and discussion is currently being prepared for submission for publication of the material. T. Tang, M. Francoeur, D. Ramanathan. The thesis author is the primary author of this material.

ABSTRACT OF THE THESIS

Neural Activity in Rat Orbitofrontal Cortex Related to Punishment and Reward

by

Tianzhi Tang

Master of Science in Biology

University of California San Diego, 2020

Professor Dhakshin Ramanathan, Chair
Professor Eric Bennett, Co-chair

Feedback processing is a key determinant of the decision-making process. During feedback processing, the outcomes of subjects' responses are evaluated based on the outcome's value and subjects' expectations. These processes inform subjects' future choices as they learn how to maximize reward and minimize punishment. Abnormalities in feedback processing are present in several psychiatric disorders, including obsessive-compulsive disorder (OCD), major depressive disorder (MDD), and substance abuse disorder (SUD).

The orbitofrontal cortex (OFC) is claimed as an important brain region in feedback processing across species. Studies in primates and rodents have mainly analyzed activities of individual neurons (single unit activity)/neuronal populations. One of the challenges in recording single unit activities is the cost of device and uncertainty of the yield and longevity of recording. In my master's project, I have developed a single unit collection device that enables affordable collection of single unit activity in rat OFC and anterior cingulate cortex for an average of 12 weeks with a range from 5 to 24 weeks. Each device costs less than $100 U.S. dollars, and the technique can be easily applied to other superficial and deep brain regions.

Using our single unit probe design, we have collected single unit activities in OFC when rats performed a go/wait task. We have found that the activity OFC neurons were modulated during the period of reward/punishment evaluation and response preparation. Our findings are consistent with previous literatures. We are in the progress of analyzing single unit activity with LFP activity through techniques such as spike-field coherence.

INTRODUCTION

The importance of feedback processing in decision-making

Decision-making is an essential and complicated process. Making choices based on perceived stimuli or environment are involved in our daily lives. The decision-making ability is impaired in several neurological and psychiatric diseases, including lesions or hemorrhage in the prefrontal cortex, Parkinson's disease, borderline personality disorder (1–3). Understanding the brain coordinates the decision-making process is directly relevant to understanding the impact of psychiatric diseases on high-order cognitive functions and developing targeted treatment.

Many steps are involved from the moment stimuli are perceived to the point where corresponding actions are executed (4). According to Wang et al. (2004), subjects need to recognize and comprehend the objective and the condition in the first place (5). Then, they would need to come up with strategies through the help of the external conditions and their own memory. After accounting for the "adequacy" of all possible choices, subjects choose one option. The result of their choices are then evaluated and encoded to inform future choices. Three common decision-making tasks used in rodent studies are delay-based, effort-based, and uncertainty-based (4). In delay-based decision-making tasks, the amount of delay in receiving the reward is typically related to reward size. In effort-based decision-making tasks, the amount of energy the subject spends correlates with the reward size. In uncertainty-based tasks, reward size could be tied to the ambiguity of rules for reward delivery.

Among all cognitive functions involved in decision-making tasks, evaluation of feedback from response is an important component in driving subjects' behaviors. Reward-based learning has been a major focus in studies on brain plasticity, attention, and motivation (6–9). Reward-

based learning also has strong clinical significance, as several studies indicated that this learning function is impaired in psychiatric disorders including Parkinson's Disease (10,11). Previous studies have identified several brain areas that play important roles in reward processing, including the prefrontal cortex and the nucleus accumbens (12–14). Specifically, the dopaminergic and glutamatergic projections to these two brain regions are thought to play a role in the processing and anticipation of reward (12).

Besides reward evaluation, error feedback is also an important component that could change future decision-making (15). Error-related learning is vital in supporting normal behaviors. In psychopathy patients, their reduced capacity to learn from punishment and aversive stimuli are believed to be associated with their impairment in making the correct choices that lead to reward (16,17). Human fMRI studies have identified that right anterior cingulate and bilateral insula are highly active when the subjects performed the wrong action(18). In a rodent error-learning study by Narayanan and Laubach (2008), rats were trained on a leverpress/delayed-releasing task (19). A significant portion of neurons in the prelimbic cortex (dmPFC) in rats are found to be positively correlated with post-error reaction time. This correlation implied a role of rat dmPFC in "retrospective memory" that could improve future task performance (19).

The role of orbitofrontal cortex in feedback processing

The orbitofrontal cortex (OFC) is recognized as a key region for feedback processing and feedback-related learning. Its importance is prominently described in studies about psychiatric disorders. Changes OFC activity is also found to be associated with drug-induced reward and craving, particularly in patients with substance abuse disorders (SUD). Human PET and fMRI studies looking at the relationship between metabolic activities and drug cravings revealed that

OFC had higher glucose metabolism in SUD patients compared to healthy control, and that OFC activity is positively correlated with methylphenidate- and alcohol- induced craving in subjects with SUD (20–22). Furthermore, changes in OFC activity is also found in human subjects with Obsessive-Compulsive Disorder (OCD), a psychiatric disorder in which patients suffer from altered responsivity to naturally existing rewards (23). Baxter et al. (1988) found that OCD patients had abnormally high metabolic rates in OFC areas (24). Many other studies have reported change in OFC grey matter sizes in patients with OCD (25). Apart from OCD, OFC is also a brain area of focus in studies related to major depressive disorder (MDD). These studies have discovered that abnormal physiological activity and the structural volume of OFC are related to major depression disorder (MDD) (25–27). In terms of their emotional processing functions, MDD patients are also found to have less metabolic activity in their OFC areas when receiving an emotional stimulus (25).

In addition to observations from human subjects, animal models are great tools to achieve deeper understanding of the functions and significance of OFC. A premise of studying OFC in animal studies is to find the equivalent of human OFC in animals including non-human primates and rodents. Previous studies have found that the primate OFC is structurally and functionally similar (28). Anatomically, both central OFC and ventromedial PFC in primates and humans include the same architectonic areas (28,29). In terms of connectivity, OFC in both humans and non-human primates are involved in two major connections: the amygdala and the lateral orbital regions (30).

There are more discrepancies between rat OFC and primate OFC. Anatomically, rat OFC only consists of agranular cortex, granular cortex is present in primate/human OFC (28). Functionally, OFC lesions in both primates and rodents compromise subjects' behavioral

flexibility in response to reward and learning of the outcome values associated with particular stimuli (31–33). However, rat OFC neurons seem encode information about the action required to obtain an outcome, a modality not seen in primate studies (28,34). Despite these distinctions, the orbitofrontal cortices in humans, primates, and rats share many similarities in connectivity and functions, justifying the attempt to study the significance of OFC in humans through primate and rodent models (28).

Rodent models present unique strengths in investigating neural changes during reward learning and processing. Tools and methods that help collect rodent electrophysiology collection have been commonly used for decades. Molecular tools, such as optogenetic manipulation and calcium imaging, have been developed for genetically modified rodent strains to allow researchers to couple behavioral testing with neuron-specific recording and control. Furthermore, behavioral training in rats has been widely performed. Rats are known to be able to learn a large variety of reward-related tasks successfully, including the go/no-go task, reversal learning task, and delay-discounting tasks (35–37).

Ample rodent studies have claimed that OFC is a major player in encoding the responses and response-based outcome anticipation. Feierstain et al. (2006) found that a in an odor-driven discrimination task, a significant portion of recorded OFC neurons were selectively active for one of the two responses rats made (38). They further claimed that this selectivity of activation is not likely stimuli dependent. In another study using odor-driven discrimination task, Schoenbaum et al. (1998) added a negative component to the reward/feedback phase (32). They discovered that around 20% of OFC neurons fired differently in prediction of a sucrose water reinforcement or a quinine water “punishment”. These findings suggest that OFC neurons are important in anticipation of reward based on subject’s responses.

OFC neurons are also claimed to play a crucial role in evaluation of properties of reward, such as probability, size, relative cost, and temporal delay. At a population level, Duuren et al. (2009) have discovered that activity of OFC neurons are related to the probability of reward delivery (33). Several studies have found that OFC lesions in rats lead to a preference of smaller, more immediate rewards over larger, delayed ones (39–41). In a lesion study by Rudebeck et al. (2006), rats were trained to choose either side of a T-maze to get one food pellet immediately, or to get ten food pellets after waiting for 15 seconds (42). Those with OFC lesions exhibited increased preferences to smaller, more immediate rewards over the alternative compared to sham control. However, their preference altered when delay was imposed on both high-value and low value rewards. These findings are consistent with the proposed hypothesis that OFC is crucial for integrating the temporal cost of the reward as part of the decision-making process in rats (42,43). By recording LFP activity in the OFC areas when rats are performing an olfactory discrimination task, Wingerden et al. (2011) found that OFC areas showed increased theta-to-gamma phase-amplitude coupling, a mechanism related to learning according to Bergmann and Born (2018), when rats performed correctly (44,45).

The advantage of associating activities of individual neurons with those from population-level

Numerous existing literatures have demonstrated the importance of OFC in feedback processing and its clinical significance through different scales of lenses. The majority of studies using animal models, as illustrated above, have been focusing on collecting and analyzing activity (action potential) of single neurons. This single-unit focus can portray modulation of individual neurons and the diversity of neurons in the brain area. On the other hand, it does not provide us

with information about the potential change in coordination among neural populations or brain areas with repeated exposure of stimuli. Human clinical studies, in contrast, tend to focus on more macroscopic scale of brain activity. This focus captures changes of activity across a larger number of brain areas and allows researchers to locate areas of particular interest. However, it can miss out detailed mechanisms behind the general changing patterns.

Associating understandings from different levels of focus can be highly advantageous. Since activities of large neural populations come from combinations of individual neuronal firing, the functions and modulations of single neurons can help explain changes of neural signal at a larger scale (46). Inversely, integrating larger-scale focus in experiments can allow inference of the downstream impacts when single neuron activities are manipulated.

To our knowledge, there has not been sufficient attention on investigating prefrontal neural activity with a multi-level approach. The few studies that attempted to examine activities of brain areas in the form of a neural network gave speculative results. As one example, Hardung et al (2017) collected single unit activities from five areas spanning the prelimbic (PL), infralimbic (IL), and ventral, medial, and lateral OFC when rats performed a behavioral inhibition task (47). They found that activities of neurons in five regions were differentially modulated across different periods of the task. Based on the types of task-modulated neurons each area has, they proposed a functional gradient of the areas in behavioral inhibition. PL is responsible for planning for future inhibition, and IL and medial OFC are responsible for both inhibition and preparation of action. Ventral OFC, on the other hand, is more responsible for initiating actions. This model can help illustrate the interaction and relationship between individual brain regions. As it's increasingly agreed upon that cognitive processes are modulated by coordination among several brain regions,

knowledge at the level of neural networks can provide more insight on the dynamics of brain functioning and malfunctioning (48,49).

In our lab's recent study, we examined the brain oscillations in multiple brain areas when rats performed Go/no-go tasks, a type of task in which subjects choose to execute an action or withhold such action based on the perceived stimuli. We found that oscillations of different frequencies (theta, alpha, and beta) dominated in cognition- and motor- related areas at different time points in the tasks. Furthermore, we found that the OFC showed increased correlation of theta activity with other cognition- and motor- related areas when rats were inhibiting their response in no-go trials, and both OFC and prelimbic cortex exhibited increased alpha correlation to the rest cognition- and reward- related areas during reward anticipation (unpublished results). Our findings had provided a comprehensive background for the neural networks active during our Go/no-go task. Further understanding of how each area modulates/ is modulated by different oscillation frequencies of the network can be achieved if we examine the single unit activities of neurons in this area.

Objectives of the thesis project

The objectives of my master's thesis project are twofold. Firstly, I seek to develop a reliable set of techniques of electrode fabrication, implantation, and spike sorting that enable collection and analysis of single unit activity in OFC and ACC neurons. Secondly, I want to characterize the roles of OFC neurons in key cognitive functions in go/wait tasks and their activities to brain oscillations to examine the two areas' roles in a neural network active crucial for decision-making and behavioral inhibition.

MATERIALS AND METHODS

Ethics statement

This research was conducted in strict accordance with the Guide for the Care and Use of Laboratory Animals of the National Institutes of Health. The protocol was approved by the San Diego VA Medical Center Institutional Animal Care and Use Committee (IACUC, Protocol Number A17-014).

Subjects

The proposed stationary electrodes were tested in 9 male Long Evans rats obtained from Charles River Laboratories. Rats were around 1-month old weighing 150g when received and were given 2 weeks to acclimate before they began behavioral training. Two rats were housed in standard plastic tubs (10 x 10.75 x 19.5 in, Allentown, NJ, USA) prior to surgery, and rats were single housed after surgery. Rats were kept on a 12h light/dark cycle (lights on at 6am) and tested during the light cycle. Food was provided ad libitum and water was restricted to 20mL/day on days with behavioral testing so that water could be used as a positive reinforcer during operant tasks. Water was unrestricted on non-training days. Rats were approximately 8 weeks old at the start of behavioral training and 3-5 months old at the start of recording. Subjects with a weight range of 300g-600g were used for implantation, at different phases during their behavioral training. Subjects with chronic implants were monitored daily for signs of infections, injuries, and bleeding. On average, rats were 7-8 months old at the conclusion of study.

Fabrication of fixed electrode arrays

Nichrome wires with a diameter of 12.7μm (Sandvik) were cut into 5-6cm segments. 30-gauge hypodermic cannulas (Mcmaster-Carr) were cut into 8-9mm sections, and the lumen was cleaned. 8 pieces of wire segments were pulled through the proximal end of a metal tube, with at least 10mm extending beyond the distal end. Wires on the distal end were carefully split into two small bundles, each with four wires (**Figure 1A**). A tiny amount of superglue (Loctite) was applied to hold the bundles separate from each other without covering the tip of the electrodes. Each bundle of four wires was split again to two bundles of two wires, and these bundles were held separate by superglue (**Figure 1B**). The distal end was then fixed to the metal cannula by superglue and was trimmed to extend 6mm beyond the cannula opening by serrated scissors (Fine Science Tools, CA, USA).

Two of these 8-wire cannulas were first grouped and glued together to form a 16-wire bundle (**Figure 1C**). Two of such bundles were then aligned and fixed together to form a big bundle with 32 wires in total, with the tips spreading across an area of approximately 1mm×1mm (**Figure 1D**). The angle of each cannula can be manually adjusted so that overlap between wires from different cannulas was kept to a minimum. A 32-channel probe was used in most surgeries, although we attempted to increase single unit collection and/or number of brain areas collected using 64-channel probes in some implantations. Two of these 32-wire bundles were used in a 64-channel probe. These two bundles can be used to target two different areas of interest; in our case, we placed one bundle in ACC and another in OFC. The horizontal and vertical distances between the two areas of interest were calculated using the rat brain atlas (50), and two 32-wire bundles were placed against each other according to the calculated distances. After the bundles were fixed with each other by viscous superglue (Loctite) and dental cement (Stoelting, IL, USA), they were mounted onto a 32-channel or 64-channel EIB board (EIB36-PTB, Neuralynx, MT, USA) using

dental cement and superglue (**Figure 1D**). Wires from the proximal ends were inserted and connected to channel holes on the board using gold pins (Neuralynx, MT, USA), and channel mapping pattern was noted. Wire tips were electroplated to an impedance of 500kOhm at 1kHz using the NanoZ impedance tester (Neuralynx, MT, USA) and gold-plating solution (Neuralynx, MT, USA). Electroplating improves the signal-to-noise ratio of recorded units by controlling the impedance. The distal ends of cannulas were cleaned using 70% ethanol and gently dried with paper tissues. Our 32-channel probe has a size of 20mm×19mm×25mm and a weight of 1.5g. The 64-channel probe has a size of 30mm×30mm×25mm and a weight of 2g.

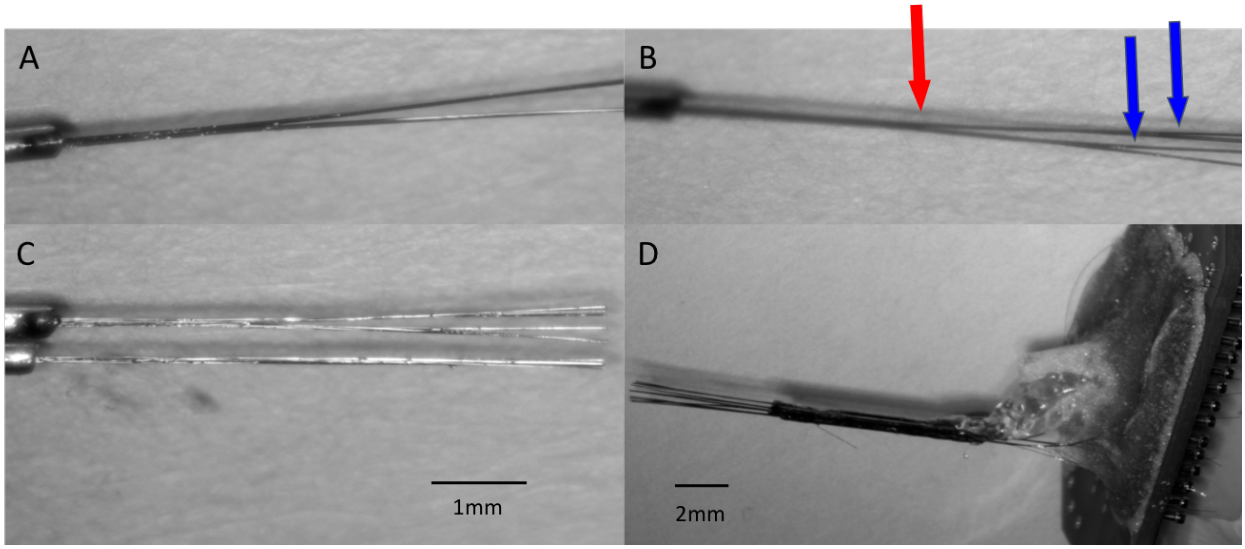

Figure 1: Fabrication of the electrodes used for implants. (A) Eight 12.7µm nichrome wires were pulled through a 9mm 30-gauge cannula, and wires were separated into bundles of four using superglue. The arrow points to the location of superglue application. (B) Each bundle of four wires were further separated into two bundles of two wires. Red arrow points to the separation in (A), while the blue arrow points to the new separation. (C) Two of these cannulas were glued together in parallel. (D) With another pair of cannulas joined together, a 32-electrode assembly is made. The 32-electrode assembly is then attached to the EIB board using dental cement and superglue.

Implantation Surgical Procedures

Stereotaxic surgery with sterile methods was used to implant fixed brush electrodes. All surgical tools were autoclaved prior to surgery. Rats were deeply anesthetized in an induction chamber with 5.0% isoflurane/ 96% room air using a low-flow anesthetic machine (Kent Scientific, CT, USA). Rats were transferred to the stereotaxic frame and 1.9-2.5% isoflurane was delivered through a nose cone with the rat in a fixed position for the remainder of surgery. A body temperature-controlled heating mat (VWR, PA, USA) was used to maintain animal temperature at 37 °C. The area of incision was cleaned with 70% ethanol and iodine solution. Lidocaine was injected (0.2cc max) to provide local anesthetic to the injection site. Incision is made to reveal skill bone and skin was kept at the periphery by four skin clamps. A ground screw (Fine Science Tools, CA, USA) (with ground wire attached with solder) was tapped into the bone posterior to lambda point on the skull, and three anchor screws were tapped into the bone at the periphery of the skull (**Figure 2A**). All screws used were self-tapping with 1.2mm diameter (Fine Science Tools, CA, USA). Screws were secured with C&B Metabond (Parkell, Inc., NY, USA) on dried skull bone. A cranial window was created with at 2.5-4.5mm anterior, 1.0-3.3mm lateral to bregma (**Figure 2B**). Creating a large enough cranial window increases flexibility during implantation, as the optimal implantation site could be hindered by blood vessels. After removal of dura, two electrode bundles were placed upright at the coordinate of anterior cingulate cortex (AP: +3.2mm, ML: +1.0mm, DV: 3.5mm), ventral orbitofrontal cortex (VO)(AP: +3.5mm; ML: +1.5mm; DV: 5.0mm), or lateral orbitofrontal cortex (LO)(AP: +3.5mm; ML: +25mm; DV: 5.0mm) (target locations variable depending on build) and inserted into the brain at a speed of 5m/s (**Figure 2C**). Super Glue was applied to seal the cranial window, and the wires and interior components were sealed and attached to the skull by Metabond (Parkell Products Inc., NY, USA) and dental cement. When

the dental cement dries, the skin is sutured closed using non-absorbable sutures (Stoelting, IL, USA). Animals are given a one-time dose of long-acting buprenorphine (72 hours) post-surgery. The rat is returned to the home cage and monitored until awake and ambulatory. A heating pad is placed under half of the home cage to prevent hypothermia during recovery. Sulfamethoxazole/Trimethoprim was given in drinking water for 7 days post-surgery, and 1.5mg/kg dexamethasone was given in drinking water for 5 days.

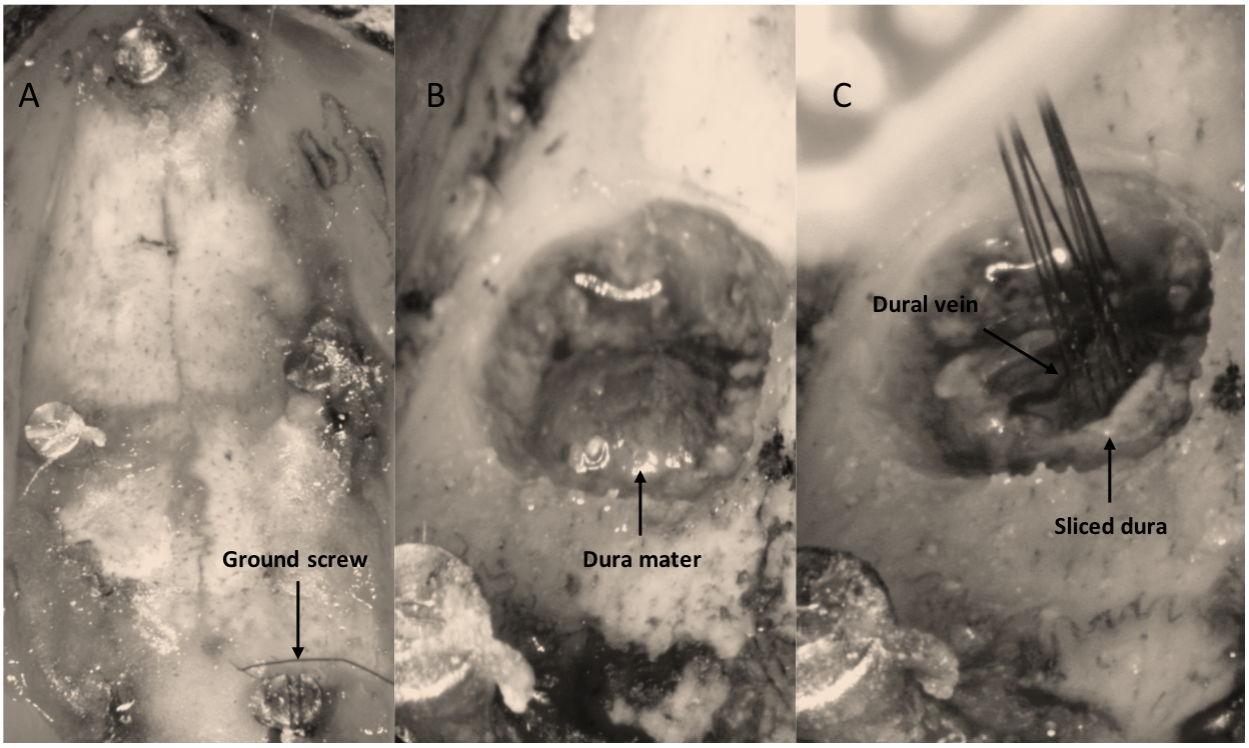

Figure 2: Surgical implantation of the fabricated probe. (A) A ground screw was put into the skull posterior and lateral to lambda. Three anchor screws were put into the lateral and anterior areas. Screws were secured with Meta-Bond and dental cement onto dry bone, and the lateral skin-skull gaps were filled with smooth dental cement. (B) A 2mm2mm craniotomy was performed anterior and lateral to bregma. Bleeding was minimized such that the exposed dura was intact. (C) Part of dura was cut open to expose an area of brain tissue with no thick blood vessels present. The electrode tips were lowered into that area.

Behavioral training

Naïve rats are first trained in a pre-training paradigm. This paradigm familiarizes them with the functions of the behavioral box. All behavioral trials were self-initiated. There are five ports on the behavioral box, and they need to reach into the middle port to initiate a trial. Then, they can get reward by going into the port to the left, or the port to the right.

After rats could perform more than 100 trials on the pre-training paradigm for 3 consecutive days, they were shifted to the actual go/wait task. In the task, rats initiate each trial, and they are instructed to either reach into an IR-activated water port within 1000ms after presentation of a "go" visual stimuli or wait for permission signaled by an auditory stimuli 1500ms after presentation of a "wait" visual stimuli. 1.5mL water will be dispensed if the rat successfully triggers the port within 1000ms of a "go" stimuli, or after the auditory cue in the wait trial. If no response is detected within 1000ms of the onset of a "go" stimuli or within 4000ms from the onset of a "wait" visual stimuli, the LED house light will flash to indicate an error in response. Premature responses in wait trials will also trigger the flashing light error signal. We first trained rats on a 50% paradigm, in which the ratio of go trials versus wait trials were 50/50. We then shifted to a 25% paradigm, in which go trials/wait trials ratio was 25/75. The number of correctly performed "go" trials (go-correct), the number of premature responses in wait trials (wait-incorrect), and the number of correctly performed "wait" trials (wait-correct), along with their time stamps, were recorded.

Analysis Electrophysiology Recording

Rats were recorded in a 6.2 × 4.7 × 6.23-inch behavioral box with a ceiling opening to allow for electrophysiology cables to move freely. The behavioral box is shielded by metal wire

meshes and powered by 24 V batteries (TalentCell PB24A1 72W battery, amazon.com) to reduce electrical (60Hz) noise. Each RHD 32-channel recording headstage is connected to a RHD SPI Interface cable (Intan Technologies, CA, USA), shielded to protect cable during recording sessions. The go and wait trials were randomized, and the ratio of two trials was set to 25:75, to encourage more learning of the wait trials. The interface cables both attach to a grounded motorized commutator (TDT, FL, USA). The signal was amplified by the PZ5 Neurodigitizer and RZ2 Bioamp Processor (TDT, FL, USA). Recorded signals were processed using Synapse software (TDT, FL, USA) at a sampling rate of 25KHz. High-pass filter was set at 300Hz and low-pass filter was set at 3000Hz. Behavioral markers were sent to the Synapse software via a LSL streaming software to integrate and store physiological and behavioral data streams. Recording sessions last 50 min. On average, each rat was recorded twice a week.

Data Analyses

Spike sorting

Recorded data were cleaned and referenced off-line using Wave_Clus v.2.5., a Matlab-based spike-sorting program (51). With this method, signals can be processed separately for each channel, or processed as polytrodes. Considering the closeness of our electrodes, we elected to process signals as polytrodes to avoid a bias cell count from units that may have been recorded on multiple channels. Electrodes in each brain area were grouped into 2 bundles of 16 electrodes during referencing, and median referencing against the 16-trode group was applied to each channel. There are three basic stages to single unit analysis: spike detection, feature extraction, and clustering (51). First, a threshold of spike detection was set at 5 times standard deviation of voltage potential in each channel (**Figure 4B,F**). Broken channels, with large impedances were sometimes

excluded from referencing or clustering. Second, Wave_Clus uses a wavelet transform to select the optimal coefficients for each of the identified spikes that give optimal separation between different clusters (51). Finally, Wave_Clus uses a nonparametric clustering algorithm, super-pragmatic clustering, to group spikes into clusters (51). Clustering of polytrodes is done by concatenating the spike shape collected in the 16 channels (52). Spikes in each polytrode group (max of 4 polytrodes), as identified by Wave_Clus, were examined manually for characteristics of single units (**Figure 4**). The distinctive clusters in each individual channel were compared across other clusters in the polytrode group and merged with those having similar spike features. For detailed steps of polytrode sorting see Swindale and Spacek (2014) (53). Spikes were considered a single unit when the average spiking rate was more than 0.5Hz across the recording session, had fewer than 1.5% inter-spike interval (ISI) violations (<3ms), when waveforms resembled action potentials as opposed to sinusoidal noise artifacts and when the cluster was distinct from other clusters in the principal component space (52,53) (**Figure 4**). Spikes meeting this criterion are counted as single units and time-locked with behavioral events (**Figure 7**). The total number of neurons sorted by the polytrode sorting algorithm in each session was recorded and compared against the number of neurons sorted in the first session of the rat.

Extraction and analysis of markers for behavioral events

Individual behavioral markers, along with its time of occurrence, were extracted through Matlab scripts. The animal's reaction time in each trial was calculated through subtracting the time point of response by the time of stimulus onset. Average and standard deviation of reaction time for go trials and wait trials were calculated in each session. The session is characterized as a

"learned session" if the average reaction time in wait trials are at least 40% higher than that of go trials. Otherwise, the session is characterized as an "unlearned session".

Categorizing and examining feedback-modulated neuronal activities

Timestamps for the onset of each go and wait trials within one session were identified. Firing rates of all identified neurons within the range from 2000ms before to 2000ms after response were extracted. Average and standard deviation of firing rates for correctly performed go trials, correct, and incorrect wait trials were calculated. Neurons with more than two standard deviations increase or decrease of average firing rates for at least 75ms compared to pre-trial baseline activity (-2000ms~-1750ms) were characterized as feedback-modulated neurons.

Histological Analyses

At completion of recording sessions wire tips were marked by passing 12A current for 10s through each channel using the Nano-Z (Neuralynx). Rats were sacrificed under deep anesthesia (100 mg/kg ketamine, 10 mg/kg xylazine IP) by transcardiac perfusion of physiological saline followed by 4% formalin. Brains were extracted and immersed in 4% formalin 24 hrs and then stored in 30% sucrose 4% formalin until ready to be sectioned. Tissue was blocked in the flat skull position using brain matrix, and sectioned frozen in the coronal plane at 50um. Brain slices of interest were stained for Nissl bodies using thionin. Tissues were examined to identify the course of electrode tracks in target brain areas. We are still in the progress of preparing histological results due to the lab closure in accordance to COVID-19 policies.

RESULTS

CHAPTER 1. Assessment of the design and implantation of the single unit probe

Since our data collection was accomplished by a customized device design with the aim of lowering the time and financial cost of fabrication, we would like to evaluate the performance of the device in terms of single unit yield, quality, longevity, and sites of implantation.

Time and cost for probe fabrication

Fabrication of a 32-wire bundle (two 32-wire bundles in a 64-channel electrode) can be finished within 2-3 hours by a trained person, while attaching and pinning of the wire bundle to the EIB board takes another 2-3 hours. The cost of each of our probes, including the wires, the pins, and the EIB board, is approximately $100. Commercially available electrodes on the other hand, typically cost more than $250 with cost of micro-drives rising above $1,000, not including the tools that help with drive assembly. In contrast, no specific assembly tools are needed for our probe. Aside from the common tweezers, our probes only need two holders that keep the electrode bundle and the EIB board stationary when fixing them together. By fixing and covering the side of the electrode attaching to the board with glue and dental cement, it becomes less likely to touch the attached wires when cleaning and implanting the probes. Note that the cost calculation does not include instruments for impedance adjustment, surgical apparatus, or tethers / recording equipment. Our 32-channel probe has a size of 20mm×19mm×25mm and a weight of 1.5-2g. The size of the total implant, including the dental cement cover, was 25mm sagittal× 20mm coronal ×20mm deep. The weight of the whole head stage was 5-6g.

Neuronal yield, longevity and waveform quality

To assess the success of our probe in vivo, we recorded from neurons in a superficial area of the brain (ACC) and deep brain structure (OFC) while rats performed a behavioral inhibition task. We collected a total of 571 units from 9 rats (average 63/ rat). An average of 6 neurons were recorded per behavioral session. 195 neurons were collected in ACC (average 65 neurons per rat) and 376 neurons from OFC (average 54 neurons per rat). The ACC neurons collected had an average firing rate of 4.8±4.6 Hz (standard deviation), while OFC neurons had an average firing rate of 4.2±4.7Hz (**Figure 3B**). We were able to achieve a 21% average yield of single unit activities per number of channels on average during the first week after post-operational recovery, and 13%-18% average yield 4-12 weeks after recovery. Change in the amount of single unit spikes across time is shown in **Figure 3A**. There is a reduction in the number of neurons sorted two weeks after the first recording, shown by a significant difference between average yield at one week after surgery compared to three weeks after surgery. The spike yield became stabilized after that initial reduction.

We were able to collect spikes with clean waveforms of action potential in both ACC (**Figure 4A-D**) and OFC (**Figure 4E-H**). In addition to meeting the criteria of having a low ISI violation (< 1.5%), most single units we collected have a visible peak in ISI histogram and produce separate clusters (k-means) in space. Spiking activity is aligned with behavior and time-locked to behavioral events. Quality of units can also be assessed by plotting PSTH and raster plots to demonstrate activity of these neurons during the Go/Wait task. This will be discussed in further details in the second section.

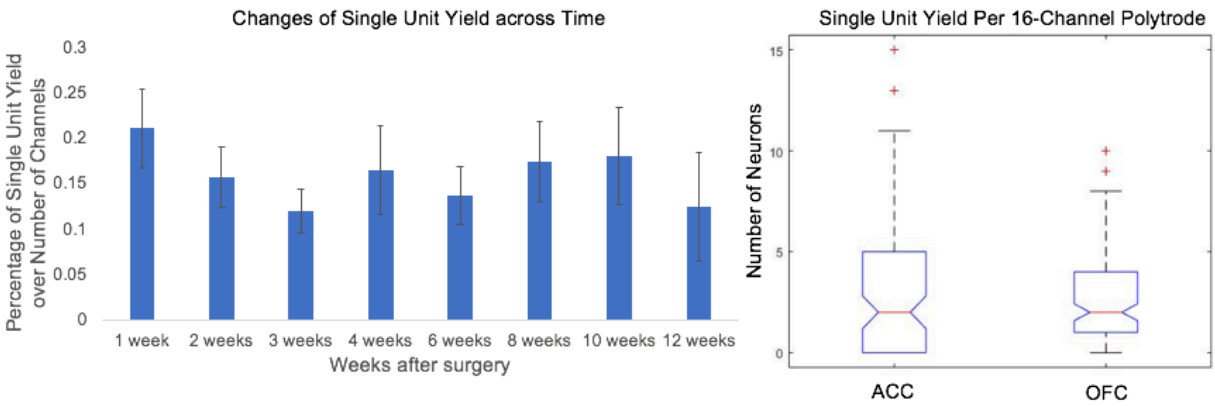

Figure 3: Longevity and Yield of our Single Unit Recording Techniques. (A) shows the average number of single neurons obtained from polytrode sorting from a 32-channel probe across 12 weeks across 7 animals. The bars showed the average number of single units obtained during the recording session in a particular week. The error bars show the standard error of the mean. The number of neurons yielded from 64-channel probes has been scaled down to 32-channel. * $p<0.05$ for Mann-Whitney U test. (B) shows the average number of neurons collected per polytrode in ACC and OFC.

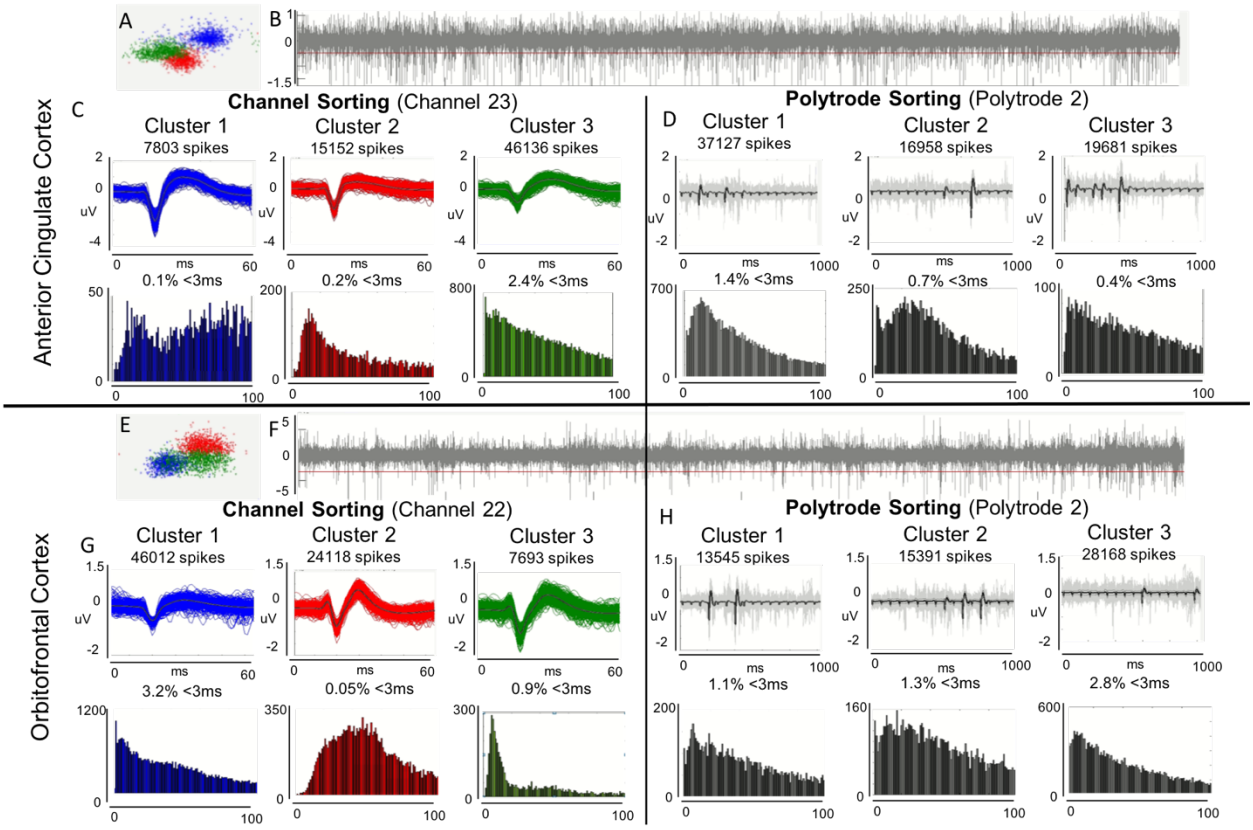

Figure 4: Example clusters produced by individual channel or polytrode sorting in ACC and OFC. Spikes detected from single channels were grouped via K-means clustering. The resulting scatterplots are shown in (A) for ACC and (E) for OFC. The bandpass-filtered time series was shown in (B) for ACC and (F) for OFC. The red horizontal line represents the 5 std threshold for spike detection. C) and G) show the waveform count,shape, ISI histogram and violation of the first three candidate clusters for the channel selected in a behavioral session using single-channel sorting. D) and H) show the cluster occurrence in each electrode, its ISI histogram and violation in the first three candidate clusters for the 16-electrode polytrode containing the electrode in C)/G).

Polytrode sorting

A comparison of single-channel spike sorting and polytrode sorting is presented in **Figure 4**. This spike cluster was detected by two of the channels shown. In single-channel sorting, this neuron may be counted twice if potential overlap was not considered. We only analyzed data from polytrode sorting but used channel sorting to visualize individual channels contributing to polytrode classification. Consistent across most sessions, there is a decrease in firing rate after time point 0, when reward is delivered. We were able to obtain raster plots for such task-modulated neurons using polytrode sorting. On average, 3.1 ± 3.4 distinct neurons can be sorted from polytrode in ACC per session, and 2.7 ± 2.5 neurons in OFC per session (**Figure 3B**).

Chapter 1 of the results and discussion is currently being prepared for submission for publication of the material. T. Tang, M. Francoeur, D. Ramanathan. The thesis author is the primary author of this material.

CHAPTER 2. Comparison and Evaluation of Single Unit Activity in Orbitofrontal Cortex in a Go/no-go Behavioral Task

Using the set of techniques described above, we were able to collect and analyze task-related single unit activities from ACC and OFC. Single units were recorded with fixed probes in 9 animals (2 targeting ACC; 6 targeting OFC; 1 targeting ACC and OFC) performing a behavioral inhibition task. On average in each rat neural activity was recorded during 10 behavioral sessions (range 5-19 sessions) across 8 weeks (range 2-24 weeks). Recording on all four animals with less than 5 weeks of data collection was terminated early due to lab shutdown. 195 neurons were collected in ACC (average 65 neurons per rat) and 376 neurons from OFC (average 54 neurons per rat). Recording from multiple brain areas shows proof of concept for my novel probe design

and demonstrates the quality of units one might expect from each brain area. The aim of my thesis is to elucidate the function of OFC neurons in brain networks during an executive function task. Therefore, in line with my research aims, my results and discuss will focus on activity of OFC neurons as opposed to ACC where we are currently still working on collecting from a larger sample size.

Behavioral performance of subjects

An illustration of the behavioral paradigm is shown in **Figure 5A.** Behavioral performance is measured by average the accuracy of go and wait trials in sessions performed by a single rat over a week. On average rats graduate from pre-training at 3 weeks. After 3 weeks rats are performing on the 25% program instead of 50%**.** According to **Figure 5B**, subjects had more than 50% accuracy in go trials in most sessions. As for wait trials, the performance slowly increased as they performed more sessions, but the variation of performance also widened. The average number of trials performed in a particular session was 150 ± 86 trials. Average rate of correct trials among all go trials is $64\%\pm25\%$. Average rate of correct trials among all wait trials is $34\% \pm 20\%$. Average reaction time in go correct trials was 805 ± 182 ms. Average reaction time in wait correct trials was 2050 ± 520 ms. Average reaction time in wait incorrect trials was 808 ± 330 ms. There is no statistical significance between reaction times of go correct and wait incorrect ($p = 0.93$). There is statistical significance of reaction times between go-correct and wait-correct, as well as wait-incorrect and wait-correct ($p < 0.01$).

The relative high accuracy of go trials and the relative low accuracy in wait trials gave us sufficient number of go-correct and wait-incorrect trials. We do not have sufficient data to analyze the behavioral inhibition component in our task. However, we are able to examine other executive

functions such as reward processing and error detection. To examine and compare OFC activity during reward and punishment evaluation, we decided to focus on response and feedback time ranges within go-correct and wait-incorrect trials.

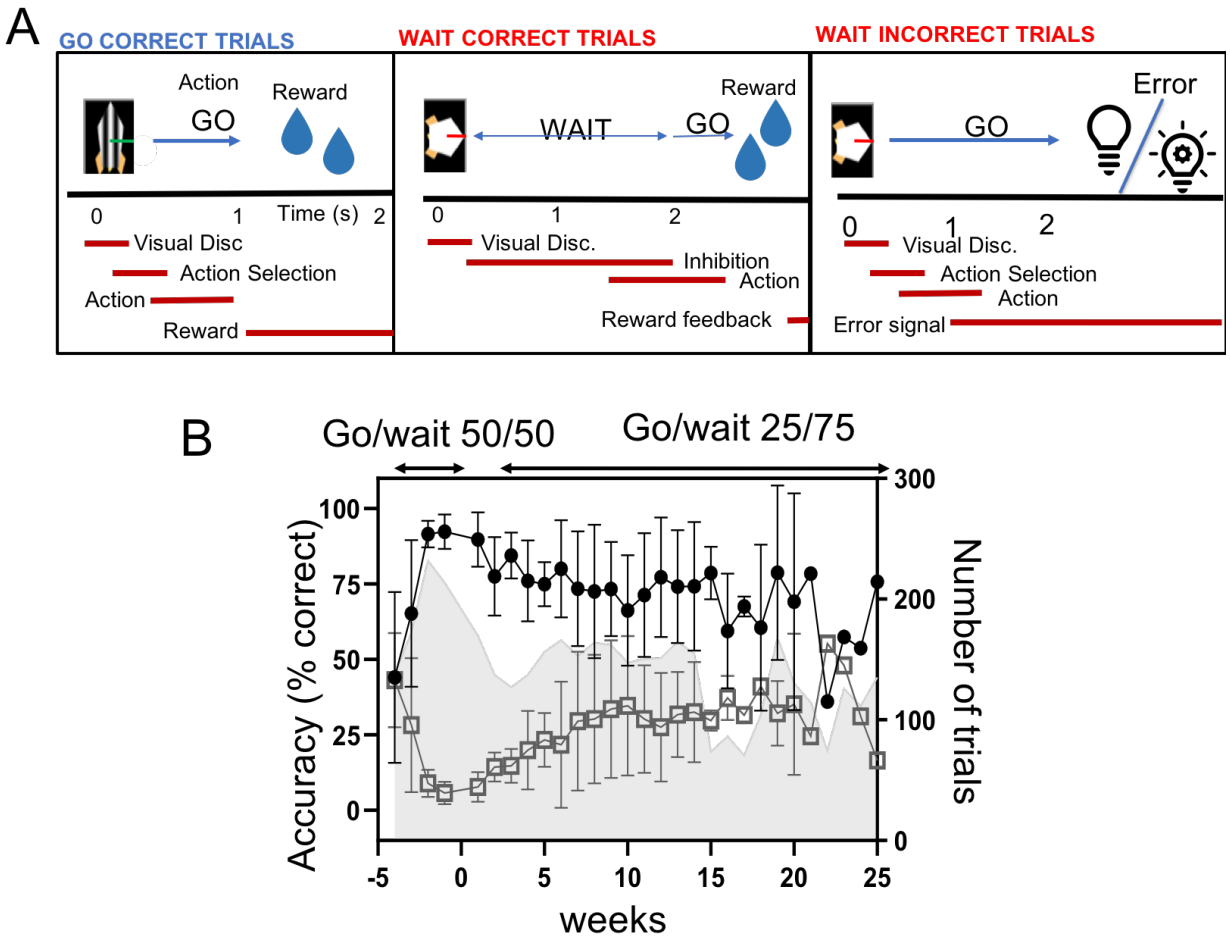

Figure 5: Behavioral paradigm and subjects' performance. In **(A),** the upper sections show presentation of cue and feedback by the behavioral training box. The lower sections show our proposed series of cognitive activities. The bar in between shows time elapse from the presentation of visual cue. **(B)** shows the accuracy of go and wait trials in all subjects with OFC single unit activity over their period of training, and the average number of trials rats performed in a session across 25 weeks of recording. Error bars represent standard deviation.

Activity of feedback-modulated neurons

Since we were interested in studying the firing of OFC neurons in feedback processing, we specifically examined feedback-modulated OFC neurons and their activities. For each neuron, the time of its action potential during individual trials (-2000ms~2000ms from time of response) was plotted in the raster plot. This time window was broken down to bins of 25ms, and the average firing rate in each bin was plotted on a peri-stimulus histogram (PSTH). To determine significant activation or suppression at certain period of time, we calculated the z-scores of average firing rate within each bin. Pre-trial activities (-2000ms~-1750ms) were used as the baseline during the normalization. We define feedback-related activity as in the time range of 500ms before response to 2000ms after the response. We identified "modulated" neurons as having significant elevation or suppression of average firing rate (> 2 standard deviations away from the pre-trial baseline) for over 75 milliseconds. We found 125 feedback-modulated neurons out of all 376 (33%) OFC neurons recorded.

Of these 125 neurons, there is a variety of ways through which neurons are modulated. 46 of these neurons (36.8%) had single unit activity associated with reward-anticipation (**Figure 6A**). These neurons show a transient but strong increase in average firing rate before the subjects' responses. 8 neurons (0.64%) are modulated by reward processing (**Figure 6B**). These neurons had strong increase of its average firing rate from baseline 200ms after the response in correct trials. Instead, this peak was absent or much weaker after response in incorrect trials. 19 neurons (15.2%) are modulated by error feedback. (**Figure 6C**). These neurons show higher post-response firing in incorrect trials versus in correct trials. Additionally, many neurons were modulated by both reward and error in the same manner. The neuron in **Figure 6D** showed suppressed activity after subjects' response, regardless of the type of feedback.

Figure 6: Four examples of OFC neurons with diverse patterns of feedback modulation. The left figure in each panel shows the raster plot and peri-stimulus histogram of neuronal activity in correct and incorrect trials. The middle and right figures show normalized activity of the same neuron in go-correct and wait-incorrect trials. Firing rate was normalized against the first 250ms of individual recording period (-2000ms~-1750ms). *: Firing rate that is more than two standard deviations higher/lower than the baseline. Time point 0 represents the time of response.

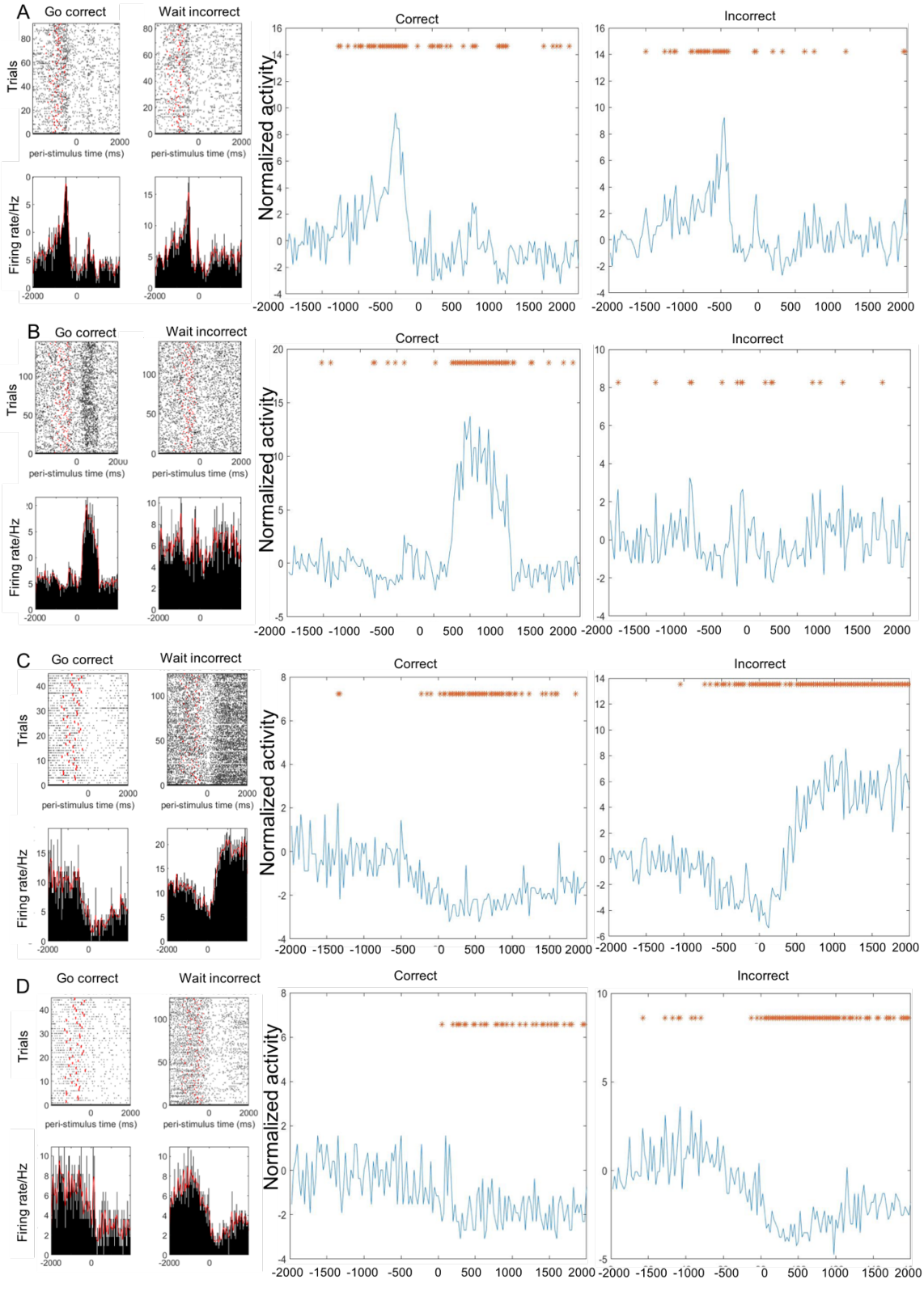
A
Go correct
Wait incorrect
Trials
peri-stimulus time (ms)
Firing rate/Hz
Correct
Incorrect
Normalized activity
B
C
D

At a population level, feedback-modulated OFC neurons exhibited different activities during reward- and error- processing. Particularly, OFC neuronal population exhibited suppressed firing in response to reward. In **Figure 7**, after the subjects made their responses, OFC activity decreased to below baseline within 500ms in both correct and incorrect trials. After 500ms, the population stayed suppressed for over 1000ms (750ms to 2000ms after response) when subjects received the reward. In contrast, the population experienced a rebound of activity back to baseline level in trials 600ms after subjects' response in an incorrect trial. Besides feedback-related activity, there is an observable increase in average population activity since 500ms before response, though not statistically significant from baseline activity.

Chapter 2 of the results and discussion is currently being prepared for submission for publication of the material. T. Tang, M. Francoeur, D. Ramanathan. The thesis author is the primary author of this material.

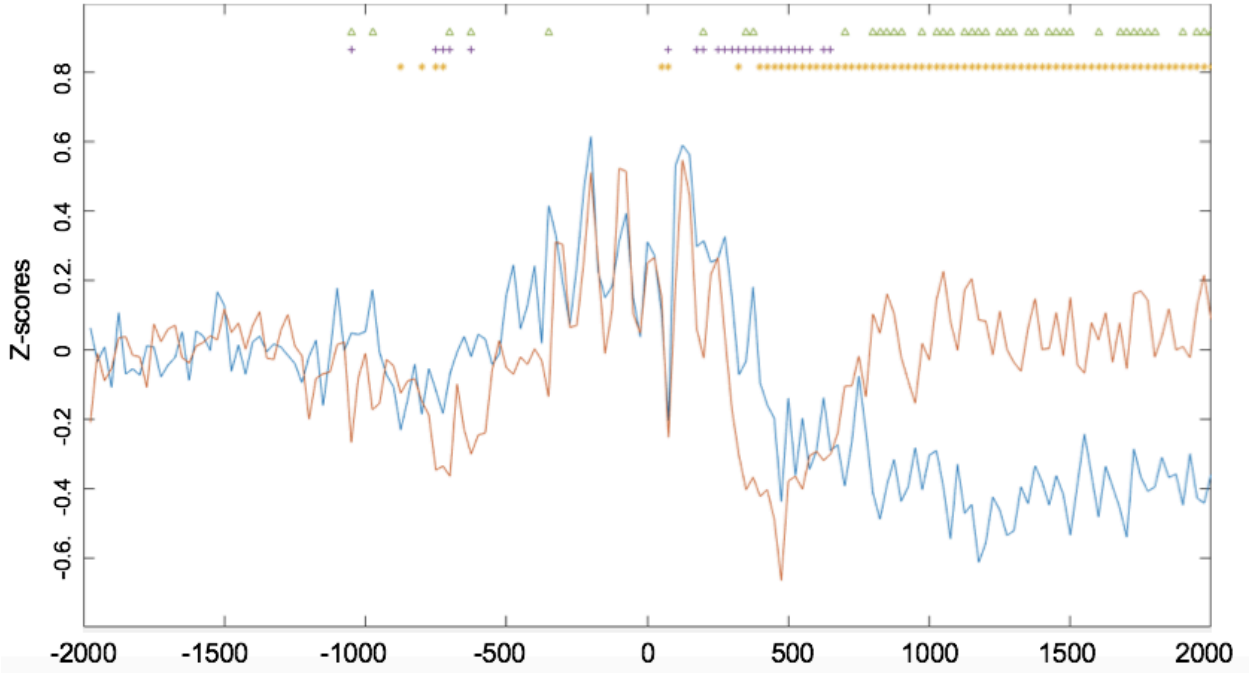

Figure 7: OFC Neurons show increased population activity during error processing. shows normalized activity (z-score) of all OFC neurons across go-correct trials (blue) and wait-incorrect trials (orange) in sessions where subjects showed discrimination between go- and wait-trial types. Activities are normalized against pre-trial baseline (-2000~-1750ms). Time point 0 represents the moment when rats reach into the port to respond. *: statistical significance of z-scores in correct trials in the corresponding bin compared to baseline. +: statistical significance of z-scores in incorrect trials in the corresponding bin compared to its baseline. Triangle: statistical significance of z-scored activity between correct and incorrect trials at the corresponding time bin. Bins with statistical significance had $p<0.05$ in Wilcoxon ranksum test.

DISCUSSION

CHAPTER 1. Evaluation of the brush-electrode single unit collecting device

Many types of electrophysiological probes have been designed for single unit collection in the past few decades (54). Novel designs often aim to increase the efficiency of spike collections. Probes such as silicon microarrays, have attempted to improve collection efficiency by increasing the number of channels available for collection (55), while probes that utilize thin wires or biocompatible insulation coating were designed in order to increase the longevity of recordings (56,57). Drivable probes may also increase the quality of units due to their ability to change the depth of electrodes to record from multiple regions (58).

Despite the new techniques developed over the recent decades, there remains no consensus on the optimal practices to achieve high-yield and long-term single unit recording. There are several challenges making stable single unit recordings from awake, behaving animals difficult over long periods of time: cost and time of probe design, tissue damage during surgical implantation, sorting techniques. Variability in probe success depends largely on the induced trauma during insertion and complicated inflammatory reactions to the foreign body (54,59). Additionally, the more sophisticated devices, such as microdrives, can be skill-demanding during fabrication and use and may require long time commitment. Additionally, location accuracy of electrode tips is difficult to estimate since the wires can drift when being moved due to rotatory forces, further complicating the quality of spike collection (60,61). The uncertainty of single unit yield makes it particularly frustrating when large amounts of money and time were spent on devices that gave poor neuronal yield or longevity. Attempting to simplify the probe fabrication

and make single unit data collection more user-friendly, we sought to offer a simple, low-cost solution to record stable units in the same brain areas over months in behaving rats.

We presented a set of fabrication, implantation, and analysis techniques that enable single unit activity collection in the anterior cingulate cortex (ACC) and orbitofrontal cortex (OFC) of rats performing a behavioral inhibition task. Our stationary probe design is affordable (<$100), takes only 4-6 hours to build, and is easily customizable to reach target brain areas. Moreover, the probe is small and light-weight, critical for long-term recordings in rats. We collected a total of 571 units from 96 behavioral sessions in 9 rats. 195 neurons were collected in ACC (average 65 neurons per rat) and 376 neurons from OFC (average 54 neurons per rat). We were able to achieve 21% average yield of single unit activities per number of channels on average during the first week after post-operational recovery, and 12-18% average yield 3 weeks after recovery. Our probe successfully collected single unit data up to 24 weeks post-surgery. Here we evaluate the success of our probe based on cost and time of build, neuronal yield and longevity, and comparison of superficial vs. deep brain areas. We took specific measures to increase neuronal yield, longevity, and quality of our data by minimizing brain damage from the probe (wire size, surgical techniques, formation of wires) and using polytrode sorting techniques.

Comparison of probe performance- yield and longevity

The current fixed brush-electrode single unit probe was developed in an attempt to simplify the device fabrication process while considering the challenges of single unit recordings and suggestions for optimization mentioned in earlier studies (54). The thin, brush-like electrodes, when not placed directly above blood vessels, were able to penetrate the brain tissue without inducing significant bleeding of adjacent blood vessels. We were able to implant 32-64 wires into

ACC/OFC due to their thinness, and achieved a similar yield (10-20%) of single unit spikes across the first four weeks compared to 32-channel silicon probes (62). We further demonstrated that our probes can collect a stable amount of single unit spikes up to 24 weeks after surgery. Kook et al. (2016) reviewed ten studies which collected single unit activities from rat motor cortex, hippocampus, and thalamus (54). These studies achieved a recording longevity of 8.9±5.6 weeks compared to our probe that achieves 8.0±6.7 weeks.

A reduction in the number of neurons collected was seen within the first two weeks after surgery, but the single neuron yields generally stabilized after the third week. This finding was consistent with the study by Huang et al. (2015) (62), which finds an initial decrease in neuronal yield the first week after implantation and stabilization afterwards. The initial decrease of neuronal yield could be due to micromotion of the electrodes in the brain tissue, macromotion of the implant or electrode bundles relative to the skull due to head movement, and corrosion of the wires by immunoreactive substances (54). Additionally, Polikov et al. (2015) find hemorrhage and edema occurring immediately after implantation do not diminish until the second to sixth weeks post implantation (59). Such recovery of the adjacent neural tissue could explain a stabilization of neuronal yield rather than a continuous decrease.

Design and fabrication to support long-term spike collection

With the goal of creating a low-cost and low-time build, we chose ultrathin nichrome wires that would minimize brain damage while still collecting a high yield of quality units. Although it is difficult to assess the degree of brain damage due to surgical implantation, the low stiffness of our thin nichrome wires could theoretically reduce shearing and shear-related inflammation of adjacent brain tissues (63). Larger diameters (>50 um) are not optimal for isolating single unit

activity. Moreover, organizing the wires in a spread-out brush formation increases the total surface area covered to minimize damage during surgical implantation.

While the electrode shape is critically important to minimize damage during implantation, other physical properties such as impedance are important in order to collect a large number of quality units. Previous studies use electrodes with an impedance as low as 80-200kOhm (64,65), while most studies aim to control the impedance in the magnitude of 1-5MOhm (66,67). Lower impedances are said to contribute to higher signal-to-noise ratio and greater area of single unit detection, however electrodes with higher impedances could amplify close-by action potentials and leave out activities of farther-away neurons to achieve easier detection and sorting (65,68). We adjusted the impedances to 550-750kOhm at 1kHz by gold-plating prior to implantation to try to reach a balance between satisfactory signal-to-noise ratio and successful spike detection and sorting. Future studies should closely examine the relationship of wire material and optimal impedance levels.

Implantation

Not only should a probe be fabricated to reduce potential tissue damage, but there are surgical techniques that can be considered to minimize bleeding during implantation (69). We made drilled areas more visible by drilling off part of the skull bone around the craniotomy site. This step facilitated the evaluation of the drill depth and helped minimize bleeding due to accidental over-drilling. It is not necessary to completely penetrate the bone while drilling the grooves, as the centerpiece can be peeled off if the surrounding bones are thin enough. Dura removal is easier in younger rats, as their dura mater is more easily penetrated and sliced.

Regarding the speed of implantation, we found that slower insertion speed was related to less hemorrhage of blood vessels at the brain surfaces. However, there were debates around whether slow or fast implantation leads to smaller damage to the neural tissues. Nicolelis et al. (2003) suggested that neural tissues could adapt to the electrode if inserted at a speed around 1-2μm/s, while Edell et al. (1992) and Campbell et al. (1991) found that inserting rapidly prevent dimpling of surrounding brain surfaces due to pressure (70–72). Additionally, keeping the head stage secured on the skull across months of recording in awake, behaving animals can be challenging. In addition to drying the skull bone with hydrogen peroxide, we tried to secure the attachment by gently abrading the surface of the skull bone before applying dental cement, so that dental cement is in contact with the actual bone tissue rather than residual fluid or skin tissue. We find that by taking simple measures to minimize bleeding and create a strong contact with bone during surgical implantation you can achieve neural activity that stabilizes ~2 weeks post-surgery that can last for up to 24 months.

Advantage of polytrode sorting

Spike sorting describes the process of clustering different potentials based on their shape and firing characteristics (52). Signals are sorted with the aim that each cluster represents spikes generated by one neuron (53). It is important to know which spike corresponds to which neurons because cells surrounding the electrode may fire in response to different stimuli, therefore driving different neural circuits and behaviors. Here, we collect data from all 32-64 channels, but elect to spike sort in polytrode groups (16 channels). The polytrode sorting algorithms were able to prevent double-counting of the same neuron and present clusters of distinct neurons for further time-locked behavioral analysis. Due to its ability to compare spike waveforms collected on different channels,

polytrode sorting is commonly used in conjunction with microelectrode arrays (MEA) (53,73). Since such sorting techniques can merge clusters across different channels with similar properties, it can be used to prevent repeated counting of the same action potential picked up by different electrodes. Using our stationary probes, we do not know how close electrodes are from each other during the recording. Polytrode sorting can thus increase the accuracy of our spike counting and sorting process by merging double-counted neurons on spatially adjacent electrodes.

Chapter 1 of the results and discussion is currently being prepared for submission for publication of the material. T. Tang, M. Francoeur, D. Ramanathan. The thesis author is the primary author of this material.

CHAPTER 2. Role of OFC neurons in reward/punishment processing

The orbitofrontal cortex is involved in facilitating decision-making processes, particularly through evaluation of rewards (33,74). Studies in humans, primates, and rodents have demonstrated that OFC lesions are linked to impaired ability in adapting behavior based on changes in the stimulus-reward association (75–77). Regarding error processing, human lateral OFC areas were found to be activated when the subjects lost in a guessing game with visual cues that maximize the probability of getting reward (78). OFC lesions in rats produced decreased avoidance from punishment even when the subjects have learned the choice associated with reward (79).

Along with the wide recognition of OFC in feedback processing, there has been more attempts to reveal the underlying mechanisms. Earlier studies in rats and monkeys have claimed that specific populations of OFC neurons selectively coded for stimuli and changed their firing according to the relationship between stimuli and outcome (80,81). The more recent studies,

however, suggested that OFC neurons respond to expectation of outcome and actual outcome (82). In a spatial decision-making task, Feierstein et al. (2006) found 41% OFC neurons were selective for one of the choices and were significantly modulated during periods of response (38). This indicated a role of OFC neuron in representing the goal and expectation of reward. Another study examined monkey OFC neurons in a paradigm where reward and no reward were given to rats in a consistent order (83). 25% of neurons selectively fired before reward delivery but not in no-reward scenarios. These studies supported OFC's function in predicting the outcomes of a specific choice or behavior (82).

OFC neurons show activity related to action-planning and outcome-prediction

Our results showed that OFC neurons are associated with response in various ways. Our findings are consistent with previous literatures. Firstly, we found 36.8% of all feedback-modulated neurons that show a transient yet strong increase in firing immediately before response in both correct and incorrect trials (**Figure 6A**). This timing represents a period when rats plan on their actions based on prediction of reward associated to the particular stimulus they received (34,36). The same study, as well as others, also reported that these outcome-predicting neurons exhibit varied patterns of post-response activity (34,84), which is consistent with our observation. 21 out of the 46 neurons (45.6%) show no significant modulation of activity in post-response period in either trials. Others show activation or suppression from baseline that may or may not be trial type dependent.

OFC neurons show reward- and punishment- specific activation

We found 8 neurons that show strong increase in activity after response in correct trials compared to incorrect trials (**Figure 6B**). Moreover, we found 19 neurons with higher activity in incorrect trials compared to baseline and the correct trials (**Figure 6C**). One interpretation of these neurons' activity is that they are selectively activated by reward and punishment. The presence of such neurons has been demonstrated in multiple previous studies. Using a go/no-go task, Tremblay and Schultz (2000) found that 36% of all task-modulated monkey OFC neurons responded specifically to delivery of rewards. In another primate study, the researchers found that 11 % of all OFC neurons encoded values of outcomes (85). The same study, however, also pointed out that these value-coding neurons are more prominent in the other brain areas, such as the anterior cingulate cortex. Therefore, even if some OFC neurons are responsible for representing outcome values, that may not be its major role.

Another interpretation for the activities of the 8 reward-activated neurons is that these neurons are responding to the error in prediction of reward. Based on the relatively poor performance of subjects in wait trials (**Figure 6B**), it is reasonable to say that they were not yet familiar with the distinction between go- and wait- trials. Since they are on a paradigm with 25/75 go/wait ratio, their chance of getting a "go" trial is less common and therefore more unexpected. The neurons that show significant increase in activity may be encoding a deviation from the most common post-response scenario. Among existing literatures, although dopaminergic circuits are often thought to be responsible for reward prediction error (RPE), it has also been reported that OFC neurons also play a role in this function across species. Sul et al. (2010) recorded OFC single unit activities in rats performing a two-armed bandit task with adjustable reward probabilities (86). 52% of all reward-modulated neurons had activities associated with positive or negative RPE. Another study reported that OFC lesions impaired dopaminergic neurons' response to both

positive and negative RPE (87). In humans, several fMRI studies discovered elevated BOLD activity in the orbitofrontal cortex when subjects received an unexpected reward (74,88). It is notable that one recent study rebutted the potential role of OFC in RPE (36). When examining OFC neuron activities in a reversal learning paradigm, they did not find neurons that had prediction error-related activity. In contrast, they only found RPE-associated activity in dopaminergic neurons. However, it was previously pointed out by Sul et al. (2010) that the reversal learning paradigm is not ideal for studying RPE, due to the infrequency of reward reversal (86). Additionally, OFC neurons might change their response too rapidly to be well-captured, compared to dopaminergic neurons (86).

OFC neurons' potential role in coding a specific brain state of feedback learning

We also found 13 neurons that were activated or suppressed after response to similar extent in both correct and incorrect trials (**Figure 6D**). These neurons could be encoding information related to feedback processing, rather than specific information about the outcome. A similar hypothesis that has been proposed states that OFC neurons in rats and humans code for an abstract state within in the behavioral task that the subject is situated (89,90). The "abstract state", as defined by Wilson (2013), refers to a representation of the general progression of certain behavioral tasks (90).

Future directions on data analysis

We are in the progress to perform more detailed statistical tests to further categorize neurons. This includes using Mann-Whitney U test to compare the normalized firing rate of defined time periods between correct and incorrect trials. We also noticed that neuronal activities

in particular time periods (for example, post-response period) were largely diverse. Many neurons show either activation or suppression immediately after response (0~500ms), while they may show another pattern in a more delayed period (1000-2000ms). There may be different information processing or neural circuits involved between these two ranges. Thus, it could be beneficial to compare the change of normalized firing rate within each time range.

As outlined in the introduction, we plan to associate single unit activity with local field potential. An important advantage of such analysis is that it helps illustrate how local activities of neurons are related to a specific frequency range of brain oscillations. Additionally, it can elucidate the impact of global oscillations on single unit activities of orbitofrontal cortex. These insights will help us understand how OFC communicates with larger neural oscillation network. The technique we are currently using is spike-field coherence (SFC) analysis. This technique has been used by several previous studies to examine modulation of information input and states of information encoding primarily in the visual and motor cortex (91–93).

Moreover, we seek to examine trial-by-trial difference and signs of learning within the same session. There are ample studies suggesting that different types of learning can occur through repeatedly performing trials within a behavior session. These include motor learning, discrimination and internal reference of stimuli, and adaptation of future choice based on feedback (94–96). Specifically, in studies focusing on trial-by-trial reward-based learning, human neurophysiology studies have found that the magnitude of EEG components could predict the change of choice in upcoming trials, while BOLD activity in parts of prefrontal cortex, cerebellum, and thalamus correlated with reaction time in a working memory stimuli identification task (96,97). During our examination of neurons' raster plots, we found that several neurons had visible trends of increase/decrease in firing. These neurons may encode, as hypothesized by Yarkoni et al. (2009),

familiarity and readiness to the task or cognitive efforts (97). We plan to analyze and compare the firing patterns of individual neurons in the first 10 trials and the last 10 trials. Differences in average firing rate will be analyzed together with reaction time for potential correlation using regression analysis.

Chapter 2 of the results and discussion is currently being prepared for submission for publication of the material. T. Tang, M. Francoeur, D. Ramanathan. The thesis author is the primary author of this material.

Bibliography

1. Ernst M, Nelson EE, McClure EB, Monk CS, Munson S, Eshel N, Zarahn E, Leibenluft E, Zametkin A, Towbin K, Blair J, Charney D, Pine D. Choice selection and reward anticipation: an fMRI study. Neuropsychologia. 2004 Jan 1;42(12):1585–97.

2. Frank MJ, Scheres A, Sherman SJ. Understanding decision-making deficits in neurological conditions: insights from models of natural action selection. Philos Trans R Soc B Biol Sci. 2007 Sep 29;362(1485):1641–54.

3. Schuermann B, Kathmann N, Stiglmayr C, Renneberg B, Endrass T. Impaired decision making and feedback evaluation in borderline personality disorder. Psychol Med. 2011 Sep;41(9):1917–27.

4. Kesner RP, Churchwell JC. An analysis of rat prefrontal cortex in mediating executive function. Neurobiol Learn Mem. 2011 Oct 1;96(3):417–31.

5. Yingxu Wang, Dong Liu, Ruhe G. Formal description of the cognitive process of decision making. In: Proceedings of the Third IEEE International Conference on Cognitive Informatics, 2004. 2004. p. 124–30.

6. Eppinger B, Hämmerer D, Li S-C. Neuromodulation of reward-based learning and decision making in human aging. Ann N Y Acad Sci. 2011 Oct;1235:1–17.

7. Doya K. Modulators of decision making. Nat Neurosci. 2008 Apr;11(4):410–6.

8. Dayan P, Balleine BW. Reward, Motivation, and Reinforcement Learning. Neuron. 2002 Oct 10;36(2):285–98.

9. Huang-Pollock CL, Mikami AY, Pfiffner L, McBurnett K. ADHD Subtype Differences in Motivational Responsivity but not Inhibitory Control: Evidence From a Reward-Based Variation of the Stop Signal Paradigm. J Clin Child Adolesc Psychol. 2007 Apr 10;36(2):127–36.

10. Perry DC, Kramer JH. Reward processing in neurodegenerative disease. Neurocase. 2015 Jan 2;21(1):120–33.

11. Kapogiannis D, Mooshagian E, Campion P, Grafman J, Zimmermann TJ, Ladt KC, Wassermann EM. Reward processing abnormalities in Parkinson's disease. Mov Disord. 2011;26(8):1451–7.

12. Lapish CC, Seamans JK, Chandler LJ. Glutamate-Dopamine Cotransmission and Reward Processing in Addiction. Alcohol Clin Exp Res. 2006;30(9):1451–65.

13. Ahn S, Phillips AG. Independent modulation of basal and feeding-evoked dopamine efflux in the nucleus accumbens and medial prefrontal cortex by the central and basolateral amygdalar nuclei in the rat. Neuroscience. 2003 Jan 15;116(1):295–305.

14. Arolfo MP, Yao L, Gordon AS, Diamond I, Janak PH. Ethanol Operant Self-Administration in Rats Is Regulated by Adenosine A2 Receptors. Alcohol Clin Exp Res. 2004;28(9):1308–16.

15. Amemiya S, Noji T, Kubota N, Nishijima T, Kita I. Noradrenergic modulation of vicarious trial-and-error behavior during a spatial decision-making task in rats. Neuroscience. 2014 Apr 18;265:291–301.

16. Borries AKL von, Brazil IA, Bulten BH, Buitelaar JK, Verkes RJ, Bruijn ERA de. Neural correlates of error-related learning deficits in individuals with psychopathy. Psychol Med. 2010 Sep;40(9):1559–68.

17. Blair RJR. Psychopathy, frustration, and reactive aggression: The role of ventromedial prefrontal cortex. Br J Psychol. 2010;101(3):383–99.

18. Menon V, Adleman NE, White C d., Glover G h., Reiss A l. Error-related brain activation during a Go/NoGo response inhibition task. Hum Brain Mapp. 2001 Mar 1;12(3):131–43.

19. Narayanan NS, Laubach M. Neuronal Correlates of Post-Error Slowing in the Rat Dorsomedial Prefrontal Cortex. J Neurophysiol. 2008 Jul;100(1):520–5.

20. Volkow ND, Wang GJ, Fowler JS, Hitzemann R, Angrist B, Gatley SJ, Logan J, Ding YS, Pappas N. Association of methylphenidate-induced craving with changes in right striato-orbitofrontal metabolism in cocaine abusers: implications in addiction. Am J Psychiatry. 1999 Jan;156(1):19–26.

21. London ED, Ernst M, Grant S, Bonson K, Weinstein A. Orbitofrontal Cortex and Human Drug Abuse: Functional Imaging. Cereb Cortex. 2000 Mar 1;10(3):334–42.

22. Claus ED, Ewing SWF, Filbey FM, Sabbineni A, Hutchison KE. Identifying Neurobiological Phenotypes Associated with Alcohol Use Disorder Severity. Neuropsychopharmacology. 2011 Sep;36(10):2086–96.

23. Koch K, Reeß TJ, Rus OG, Gürsel DA, Wagner G, Berberich G, Zimmer C. Increased Default Mode Network Connectivity in Obsessive–Compulsive Disorder During Reward Processing. Front Psychiatry [Internet]. 2018 [cited 2020 Jul 4];9. Available from: https://www.frontiersin.org/articles/10.3389/fpsyt.2018.00254/full

24. Baxter LR, Schwartz JM, Mazziotta JC, Phelps ME, Pahl JJ, Guze BH, Fairbanks, L. Cerebral glucose metabolic rates in nondepressed patients with obsessive-compulsive disorder. Am J Psychiatry. 1988;145(12):1560–3.

25. Fettes P, Schulze L, Downar J. Cortico-Striatal-Thalamic Loop Circuits of the Orbitofrontal Cortex: Promising Therapeutic Targets in Psychiatric Illness. Front Syst Neurosci [Internet]. 2017 Apr 27 [cited 2019 Dec 16];11. Available from: https://www.ncbi.nlm.nih.gov/pmc/articles/PMC5406748/

26. Drevets WC. Orbitofrontal Cortex Function and Structure in Depression. Ann N Y Acad Sci. 2007;1121(1):499–527.

27. Goldstein RZ, Volkow ND. Dysfunction of the prefrontal cortex in addiction: neuroimaging findings and clinical implications. Nat Rev Neurosci. 2011 Nov;12(11):652–69.

28. Wallis JD. Cross-species studies of orbitofrontal cortex and value-based decision-making. Nat Neurosci. 2012 Jan;15(1):13–9.

29. Mackey S, Petrides M. Architectonic mapping of the medial region of the human orbitofrontal cortex by density profiles. Neuroscience. 2009 Mar 31;159(3):1089–107.

30. Croxson PL, Johansen-Berg H, Behrens TEJ, Robson MD, Pinsk MA, Gross CG, Richter W, Richter M, Kastner S, Rushworth MFS. Quantitative Investigation of Connections of the Prefrontal Cortex in the Human and Macaque using Probabilistic Diffusion Tractography. J Neurosci. 2005 Sep 28;25(39):8854–66.

31. Burke KA, Franz TM, Miller DN, Schoenbaum G. The role of the orbitofrontal cortex in the pursuit of happiness and more specific rewards. Nature. 2008 Jul 17;454(7202):340–4.

32. Schoenbaum G, Chiba AA, Gallagher M. Orbitofrontal cortex and basolateral amygdala encode expected outcomes during learning. Nat Neurosci. 1998 Jun;1(2):155–9.

33. Duuren E van, Plasse G van der, Lankelma J, Joosten RNJMA, Feenstra MGP, Pennartz CMA. Single-Cell and Population Coding of Expected Reward Probability in the Orbitofrontal Cortex of the Rat. J Neurosci. 2009 Jul 15;29(28):8965–76.

34. Schoenbaum G, Setlow B, Saddoris MP, Gallagher M. Encoding Predicted Outcome and Acquired Value in Orbitofrontal Cortex during Cue Sampling Depends upon Input from Basolateral Amygdala. Neuron. 2003 Aug 28;39(5):855–67.

35. Berditchevskaia A, Cazé RD, Schultz SR. Performance in a GO/NOGO perceptual task reflects a balance between impulsive and instrumental components of behaviour. Sci Rep. 2016 07;6:27389.

36. Stalnaker TA, Liu T-L, Takahashi YK, Schoenbaum G. Orbitofrontal neurons signal reward predictions, not reward prediction errors. Neurobiol Learn Mem. 2018 Sep 1;153:137–43.

37. Churchwell JC, Morris AM, Heurtelou NM, Kesner RP. Interactions between the prefrontal cortex and amygdala during delay discounting and reversal. Behav Neurosci. 2009;123(6):1185–96.

38. Feierstein CE, Quirk MC, Uchida N, Sosulski DL, Mainen ZF. Representation of Spatial Goals in Rat Orbitofrontal Cortex. Neuron. 2006 Aug 17;51(4):495–507.

39. Mar AC, Walker ALJ, Theobald DE, Eagle DM, Robbins TW. Dissociable Effects of Lesions to Orbitofrontal Cortex Subregions on Impulsive Choice in the Rat. J Neurosci. 2011 Apr 27;31(17):6398–404.

40. Pais-Vieira M, Lima D, Galhardo V. Orbitofrontal cortex lesions disrupt risk assessment in a novel serial decision-making task for rats. Neuroscience. 2007 Mar 2;145(1):225–31.

41. Mobini S, Body S, Ho M-Y, Bradshaw C, Szabadi E, Deakin J, Anderson I. Effects of lesions of the orbitofrontal cortex on sensitivity to delayed and probabilistic reinforcement. Psychopharmacology (Berl). 2002 Mar 1;160(3):290–8.

42. Rudebeck PH, Walton ME, Smyth AN, Bannerman DM, Rushworth MFS. Separate neural pathways process different decision costs. Nat Neurosci. 2006 Sep;9(9):1161–8.

43. Wallis JD. Orbitofrontal Cortex and Its Contribution to Decision-Making. Annu Rev Neurosci. 2007 Jun 28;30(1):31–56.

44. Wingerden M van, Meij R van der, Kalenscher T, Maris E, Pennartz CMA. Phase-Amplitude Coupling in Rat Orbitofrontal Cortex Discriminates between Correct and Incorrect Decisions during Associative Learning. J Neurosci. 2014 Jan 8;34(2):493–505.

45. Bergmann TO, Born J. Phase-Amplitude Coupling: A General Mechanism for Memory Processing and Synaptic Plasticity? Neuron. 2018 Jan 3;97(1):10–3.

46. Bassett DS, Zurn P, Gold JI. On the nature and use of models in network neuroscience. Nat Rev Neurosci. 2018 Sep;19(9):566.

47. Hardung S, Epple R, Jäckel Z, Eriksson D, Uran C, Senn V, Gibor L, Yizhar O, Diester I. A Functional Gradient in the Rodent Prefrontal Cortex Supports Behavioral Inhibition. Curr Biol. 2017 Feb 20;27(4):549–55.

48. Le Van Quyen M. Disentangling the dynamic core: a research program for a neurodynamics at the large-scale. Biol Res. 2003;36(1):67–88.

49. de Haan W, Pijnenburg YA, Strijers RL, van der Made Y, van der Flier WM, Scheltens P, Stam CJ. Functional neural network analysis in frontotemporal dementia and Alzheimer's disease using EEG and graph theory. BMC Neurosci. 2009 Aug 21;10(1):101.

50. The Rat Brain in Stereotaxic Coordinates - 7th Edition [Internet]. [cited 2020 Mar 21]. Available from: https://www.elsevier.com/books/the-rat-brain-in-stereotaxic-coordinates/paxinos/978-0-12-391949-6

51. Quiroga RQ, Nadasdy Z, Ben-Shaul Y. Unsupervised Spike Detection and Sorting with Wavelets and Superparamagnetic Clustering. Neural Comput. 2004 Aug;16(8):1661–87.

52. Rey HG, Pedreira C, Quian Quiroga R. Past, present and future of spike sorting techniques. Brain Res Bull. 2015 Oct 1;119:106–17.

53. Swindale NV, Spacek MA. Spike sorting for polytrodes: a divide and conquer approach. Front Syst Neurosci [Internet]. 2014 [cited 2020 Apr 2];8. Available from: https://www.frontiersin.org/articles/10.3389/fnsys.2014.00006/full

54. Kook G, Lee SW, Lee HC, Cho I-J, Lee HJ. Neural Probes for Chronic Applications. Micromachines. 2016 Oct;7(10):179.

55. Buzsáki G, Stark E, Berényi A, Khodagholy D, Kipke DR, Yoon E, Wise KD. Tools for Probing Local Circuits: High-Density Silicon Probes Combined with Optogenetics. Neuron. 2015 Apr 8;86(1):92–105.

56. Karumbaiah L, Saxena T, Carlson D, Patil K, Patkar R, Gaupp EA, Betancur M, Stanley GB, Carin L, Bellamkonda RV. Relationship between intracortical electrode design and chronic recording function. Biomaterials. 2013 Nov;34(33):8061–74.

57. Seymour JP, Kipke DR. Neural probe design for reduced tissue encapsulation in CNS. Biomaterials. 2007 Sep;28(25):3594–607.

58. Fee MS, Leonardo A. Miniature motorized microdrive and commutator system for chronic neural recording in small animals. J Neurosci Methods. 2001 Dec 15;112(2):83–94.

59. Polikov VS, Tresco PA, Reichert WM. Response of brain tissue to chronically implanted neural electrodes. J Neurosci Methods. 2005 Oct 15;148(1):1–18.

60. Yang S, Cho J, Lee S, Park K, Kim J, Huh Y, Yoon E, Shin, H. Feedback controlled piezo-motor microdrive for accurate electrode positioning in chronic single unit recording in behaving mice. J Neurosci Methods. 2011 Feb 15;195(2):117–27.

61. Polo-Castillo LE, Villavicencio M, Ramírez-Lugo L, Illescas-Huerta E, Moreno MG, Ruiz-Huerta L, Gutierrez R, Bayon F, Ruiz A. Reimplantable Microdrive for Long-Term Chronic Extracellular Recordings in Freely Moving Rats. Front Neurosci [Internet]. 2019 [cited 2020 May 24];13. Available from: https://www.frontiersin.org/articles/10.3389/fnins.2019.00128/full

62. Huang W-C, Lai H-Y, Kuo L-W, Liao C-H, Chang P-H, Liu T-C, Chen S-Y, Chen Y-Y. Multifunctional 3D Patternable Drug-Embedded Nanocarrier-Based Interfaces to Enhance Signal Recording and Reduce Neuron Degeneration in Neural Implantation. Adv Mater. 2015;27(28):4186–93.

63. Bae WJ, Ruddy BP, Richardson AG, Hunter IW, Bizzi E. Cortical recording with polypyrrole microwire electrodes. In: 2008 30th Annual International Conference of the IEEE Engineering in Medicine and Biology Society. 2008. p. 5794–7.

64. Nordhausen CT, Maynard EM, Normann RA. Single unit recording capabilities of a 100 microelectrode array. Brain Res. 1996;12.

65. Kim D-H, Richardson-Burns S, Hendricks J, Sequera C, Martin D. Effect of Immobilized Nerve Growth Factor (NGF) on Conductive Polymers: Electrical Properties and Cellular Response. Adv Funct Mater. 2006 Jan 1;17:79–86.

66. Humphrey DR, Schmidt EM. Extracellular Single-Unit Recording Methods. In: Boulton AA, Baker GB, Vanderwolf CH, editors. Neurophysiological Techniques: Applications to Neural Systems [Internet]. Totowa, NJ: Humana Press; 1990 [cited 2020 May 9]. p. 1–64. (Neuromethods). Available from: https://doi.org/10.1385/0-89603-185-3:1

67. Johnson MD, Otto KJ, Kipke DR. Repeated voltage biasing improves unit recordings by reducing resistive tissue impedances. IEEE Trans Neural Syst Rehabil Eng. 2005 Jun;13(2):160–5.

68. Obien MEJ, Deligkaris K, Bullmann T, Bakkum DJ, Frey U. Revealing neuronal function through microelectrode array recordings. Front Neurosci [Internet]. 2015 [cited 2020 May 24];8. Available from: https://www.frontiersin.org/articles/10.3389/fnins.2014.00423/full

69. Gage GJ, Stoetzner CR, Richner T, Brodnick SK, Williams JC, Kipke DR. Surgical implantation of chronic neural electrodes for recording single unit activity and electrocorticographic signals. J Vis Exp JoVE. 2012 Feb 24;(60).

70. Nicolelis MAL, Dimitrov D, Carmena JM, Crist R, Lehew G, Kralik JD, Wise SP. Chronic, multisite, multielectrode recordings in macaque monkeys. Proc Natl Acad Sci. 2003 Sep 16;100(19):11041–6.

71. Edell DJ, Toi VV, McNeil VM, Clark LD. Factors influencing the biocompatibility of insertable silicon microshafts in cerebral cortex. IEEE Trans Biomed Eng. 1992 Jun;39(6):635–43.

72. Campbell PK, Jones KE, Huber RJ, Horch KW, Normann RA. A silicon-based, three-dimensional neural interface: manufacturing processes for an intracortical electrode array. IEEE Trans Biomed Eng. 1991 Aug;38(8):758–68.

73. Swindale NV, Spacek MA. Spike detection methods for polytrodes and high density microelectrode arrays. J Comput Neurosci. 2015 Apr 1;38(2):249–61.

74. O'Doherty J, Kringelbach ML, Rolls ET, Hornak J, Andrews C. Abstract reward and punishment representations in the human orbitofrontal cortex. Nat Neurosci. 2001 Jan;4(1):95–102.

75. Chudasama Y, Robbins TW. Dissociable Contributions of the Orbitofrontal and Infralimbic Cortex to Pavlovian Autoshaping and Discrimination Reversal Learning: Further Evidence for the Functional Heterogeneity of the Rodent Frontal Cortex. J Neurosci. 2003 Sep 24;23(25):8771–80.

76. Rolls ET, Critchley HD, Mason R, Wakeman EA. Orbitofrontal cortex neurons: role in olfactory and visual association learning. J Neurophysiol. 1996 May;75(5):1970–81.

77. Izquierdo A, Suda RK, Murray EA. Bilateral Orbital Prefrontal Cortex Lesions in Rhesus Monkeys Disrupt Choices Guided by Both Reward Value and Reward Contingency. J Neurosci. 2004 Aug 25;24(34):7540–8.

78. Elliott R, Agnew Z, Deakin JFW. Hedonic and Informational Functions of the Human Orbitofrontal Cortex. Cereb Cortex. 2010 Jan 1;20(1):198–204.

79. Jean-Richard-Dit-Bressel P, McNally GP. Lateral, not medial, prefrontal cortex contributes to punishment and aversive instrumental learning. Learn Mem Cold Spring Harb N. 2016;23(11):607–17.

80. Thorpe SJ, Rolls ET, Maddison S. The orbitofrontal cortex: Neuronal activity in the behaving monkey. Exp Brain Res. 1983 Jan 1;49(1):93–115.

81. Rolls ET, Hornak J, Wade D, McGrath J. Emotion-related learning in patients with social and emotional changes associated with frontal lobe damage. J Neurol Neurosurg Psychiatry. 1994 Dec 1;57(12):1518–24.

82. SCHOENBAUM G, SADDORIS MP, STALNAKER TA. Reconciling the Roles of Orbitofrontal Cortex in Reversal Learning and the Encoding of Outcome Expectancies. Ann N Y Acad Sci. 2007 Dec;1121:320–35.

83. Hikosaka K, Watanabe M. Delay Activity of Orbital and Lateral Prefrontal Neurons of the Monkey Varying with Different Rewards. Cereb Cortex. 2000 Mar 1;10(3):263–71.

84. Schoenbaum G, Chiba AA, Gallagher M. Neural Encoding in Orbitofrontal Cortex and Basolateral Amygdala during Olfactory Discrimination Learning. J Neurosci. 1999 Mar 1;19(5):1876–84.

85. Kennerley SW, Wallis JD. Evaluating choices by single neurons in the frontal lobe: outcome value encoded across multiple decision variables. Eur J Neurosci. 2009;29(10):2061–73.

86. Sul JH, Kim H, Huh N, Lee D, Jung MW. Distinct Roles of Rodent Orbitofrontal and Medial Prefrontal Cortex in Decision Making. Neuron. 2010 May 13;66(3):449–60.

87. Takahashi YK, Roesch MR, Wilson RC, Toreson K, O'Donnell P, Niv Y, Schoenbaum G. Expectancy-related changes in firing of dopamine neurons depend on orbitofrontal cortex. Nat Neurosci. 2011 Oct 30;14(12):1590–7.

88. Berns GS, McClure SM, Pagnoni G, Montague PR. Predictability Modulates Human Brain Response to Reward. J Neurosci. 2001 Apr 15;21(8):2793–8.

89. Hampton AN, Bossaerts P, O'Doherty JP. The Role of the Ventromedial Prefrontal Cortex in Abstract State-Based Inference during Decision Making in Humans. J Neurosci. 2006 Aug 9;26(32):8360–7.

90. Wilson RC, Takahashi YK, Schoenbaum G, Niv Y. Orbitofrontal Cortex as a Cognitive Map of Task Space. Neuron. 2014 Jan 22;81(2):267–79.

91. An J, Yadav T, Hessburg JP, Francis JT. Reward Expectation Modulates Local Field Potentials, Spiking Activity and Spike-Field Coherence in the Primary Motor Cortex. eNeuro [Internet]. 2019 Jun 25 [cited 2020 Jul 2];6(3). Available from: https://www.ncbi.nlm.nih.gov/pmc/articles/PMC6595440/

92. Womelsdorf T, Fries P, Mitra PP, Desimone R. Gamma-band synchronization in visual cortex predicts speed of change detection. Nature. 2006 Feb 9;439(7077):733–6.

93. Fries P, Reynolds JH, Rorie AE, Desimone R. Modulation of Oscillatory Neuronal Synchronization by Selective Visual Attention. Science. 2001 Feb 23;291(5508):1560–3.

94. Gentili R, Han CE, Schweighofer N, Papaxanthis C. Motor Learning Without Doing: Trial-by-Trial Improvement in Motor Performance During Mental Training. J Neurophysiol. 2010 Jun 10;104(2):774–83.

95. Dyjas O, Bausenhart KM, Ulrich R. Trial-by-trial updating of an internal reference in discrimination tasks: Evidence from effects of stimulus order and trial sequence. Atten Percept Psychophys. 2012 Nov 1;74(8):1819–41.

96. Philiastides MG, Biele G, Vavatzanidis N, Kazzer P, Heekeren HR. Temporal dynamics of prediction error processing during reward-based decision making. NeuroImage. 2010 Oct 15;53(1):221–32.

97. Yarkoni T, Barch DM, Gray JR, Conturo TE, Braver TS. BOLD Correlates of Trial-by-Trial Reaction Time Variability in Gray and White Matter: A Multi-Study fMRI Analysis. PLOS ONE. 2009 Jan 23;4(1):e4257.